Throughfall and stemflow chemical dynamics of Satoyama, a traditional secondary forest system under threat in Japan

Asaoka, Satoshi ; Sumikawa, Fuyuhiko ; Watanabe, Yoshifumi ; Jadoon, Waqar Azeem ; Ohno, Masaki ; Shutoh, Nobumichi ; Wakamatsu, Yuki ;…

(Citation)
Journal of Forestry Research,33(3):813-826

(Issue Date)
2021-11-27

(Resource Type)
journal article

(Version)
Accepted Manuscript

(URL)
https://hdl.handle.net/20.500.14094/90008822

Throughfall and stemflow chemical dynamics of Satoyama, traditional secondary forest systems under threat in Japan

Satoshi ASAOKA[1,2]*, Fuyuhiko SUMIKAWA[3], Yoshifumi WATANABE[3],
Waqar Azeem JADOON[4], Masaki OHNO[5], Shuto NOBUMICHI[6],
Yuki WAKAMATSU[7], Lawrence M. LIAO[1],
Akane KANAZAWA[3], Yuka SATO[3], Natsumi FUJIWARA[3]

[1] Graduate School of Integrated Sciences for Life, Hiroshima University, 1-4-4 Kagamiyama, Higashi-Hiroshima, 739-8528, Japan

[2] Research Center for Inland Seas, Kobe University, 5-1-1 Fukaeminami, Higashinada, Kobe, 658-0022, Japan

[3] Naragakuen Senior High School, 430 Yamada, Yamatokoriyama, Nara, 639-1093, Japan

[4] Department of Environmental Sciences, Faculty of Sciences, Hazara University, Mansehra, Khyber, Pakhtunkhwa, Pakistan

[5] Niigata University of Pharmacy and Applied Life Sciences, 265-1 Higashijima, Akiha, Niigata, 956-8603, Japan

[6] Faculty of Science and Engineering, Kindai University, 3-4-1 Kowakae, Higashi-Osaka, Osaka, 577-8502, Japan

[7] Department of Maritime Science and Technology, Japan Coast Guard Academy, 5 Wakaba, Kure, Hiroshima, 737-8512, Japan

***Corresponding author:** Dr. Satoshi Asaoka, Graduate School of Integrated Sciences for Life, Hiroshima University, 1-4-4 Kagamiyama, Higashi-Hiroshima, 739-8528, Japan

Tel. & Fax: +81-82-424-7945, Email: stasaoka@hiroshima-u.ac.jp

Abstract

The term 'Satoyama' refers to traditional and unique secondary forests in Japan that occupy intermediate zones between villages ('sato') and hills or mountains ('yama'). Satoyama landscapes help sustain both ecosystem services and the diversity of secondary natural environments. As Japan relies more heavily on foreign timber imports, the traditional role of Satoyama in providing forest products has diminished and this has led to abandonment and poor management of the forests. We investigated the chemical behaviors of cations, anions, and dissolved organic matter in throughfall and stemflow collected from one such threatened Satoyama system in central Japan. From autumn to winter, the atmospheric deposition of sulfate and nitrate was 2.5–6.0 times higher compared to summer due to the intrusion of air mass from the Asian continent. The dissolved organic matter in the throughfall and stemflow was composed mainly of humic substances and protein derivatives. The deposition fluxes of DOC from the throughfalls (7.31–10.1 g m^{-2} y^{-1}) and stemflow (1.79–3.84 g m^{-2} y^{-1}) obtained in this study were within the range seen in temperate forests as obtained by previous studies. The deposition flux of sulfate in the Satoyama forest was low compared to other forest types. This is because canopy interaction in Satoyama forests was lower, suggesting higher canopy openness than in primary forests. In our estimation, if a shift from a mixed species Satoyama forest into a conifer-dominated forest occurs after

mass mortality of oak trees, the deposition flux of DOC and K^+ might decrease 33% and 62%, respectively, while NO_3^- might increase 20%. In the near future, the degradation of Satoyama landscapes might change DOC and nitrogen loads, resulting to imbalances in river-ocean linkages affecting forested catchments and aquatic ecosystems in Japan.

Key Words

atmospheric deposition; dissolved organic matter; humic substance; mass mortality; oak trees; SDGs

1. Introduction

Japan has one of the highest forest ratios in the world with forests comprising 68.2% of the country's land area (FAO, 2005). The Japanese word 'Satoyama' refers to forests at the border of or in intermediate zones between one or more villages ('sato') and a hill or mountain ('yama'), representing a common, traditional and rural landscape in Japan. The Satoyama landscape is composed of several habitat types such as paddy fields, secondary forests and grasslands, ponds, and streams which are maintained by human activities. Its upkeep is closely linked with supporting livelihoods and agricultural production consistent with maintaining sustainable ecosystem services and the natural diversity of the secondary environments (Takeuchi, 2010; Kamiyama et al., 2016). In essence, high biodiversity is sustained by sound anthropogenic activities related to agriculture (Katoh et al., 2009). Cultivated trees in the Satoyama are cut every 15–30 years to obtain timber for building materials, bed logs for cultivating mushrooms, charcoal production, and other wood-derived products (Katoh et al., 2009; Gan and Tsing, 2018). After clearcutting, trees regenerate from the stumps so that the forests are maintained (Washitani, 2001). However, Japan currently depends on imports for most of its timber needs, and thus, the trees in Satoyama forests have been largely abandoned without management. Furthermore, increasing urbanization saw a declining need for fuelwood while the rapidly aging society contributed to the decline of

79 interest in the maintenance of Satoyama forests (Jiao et al., 2019). Consequently, the
80 deterioration of the Satoyama triggered a domino effect of biodiversity decline due to the
81 simplification of the forest structure, mass mortality of oak and pine trees, rapid expansion
82 of bamboo forests and increasing landslides (Katoh et al., 2009; Indrawan et al., 2014; Ito,
83 2016; Koganezawa, 2016; Kamada et al., 2017; Nakajima, 2019). Therefore, the traditional
84 Japanese Satoyama is now facing a serious crisis. Globally, the deterioration of forests
85 including the mass mortality of oak trees have become serious environmental issues in the
86 USA, Italy and Switzerland (Dey and Schweitzer et al., 2018; Bendixsen et al., 2015;
87 Colangelo et al., 2018; Etzold et al., 2019). As forested catchments have been tagged as
88 primary sources of nutrients and dissolved organic matter (DOM) for aquatic systems, the
89 intimate link between upland areas and coastal areas is further emphasized. The river-ocean
90 linkages involving nutrients and DOM are critical particularly those involving massive
91 terrigenous inputs from large river systems such as the Amazon river and Changjiang river,
92 China (Gomes et al., 2018) and the Congo River (Holtvoeth et al., 2003), sometimes
93 affecting cross-border bodies of water. Hence, river-ocean linkages have shown that coastal
94 ecosystems are significantly affected by terrigenous nutrients and other material inputs as
95 well as by carbon cycling (Cao et al., 2018; Muller, 2018; Häder and Barnes, 2019).
96 Therefore, the deterioration of secondary forests such as those found in Satoyama will

97 directly affect the fate of nutrients and DOM and further change the dynamics of river-ocean
98 linkages. In Japan, the impact will be strongly felt as Satoyama landscapes comprise
99 approximately 40% of country's land area. However, nutrient and DOM dynamics in the
100 Satoyama are not fully understood. Therefore, the purposes of this study are (1) to
101 characterize the chemical composition of anions, cations, and dissolved organic carbon
102 (DOC) of throughfall and stemflow in a typical Satoyama forest facing deterioration and (2)
103 to clarify the effect of the any large-scale change of tree species composition in Satoyama
104 forests on the change in deposition flux of nutrients and DOM and subsequent changes in
105 river-ocean linkages.
106
107 **2. Materials and Methods**
108 *2.1. Study site*
109 We collected data on gross rainfall, throughfall, and stemflow at a Satoyama site, a mixed
110 forest area of 70,000 m^2 located in the campus of Naragakuen Junior and Senior High School,
111 Nara prefecture, Japan (34.63400°N, 135.73515°W; **Fig. 1**). The soil in the study site is
112 classified as brown forest soil. The forest was mainly composed of Japanese red pine (*Pinus*
113 *densiflora*) and Konara oak (*Quercus serrata*) which are used to produce firewood and bed
114 logs for cultivating mushrooms before the secondary deforestation in the 1960s. After the

115 1960s, the tree species composition of tree species in the secondary forest was limited to
116 only the Japanese red pine, Konara oak and the Japanese cypress (*Chamaecyparis obtusa*).
117 Currently, the deteriorated forest is maintained by the local high school for Satoyama
118 concept education and promotion. However, mass mortality of Japanese oak trees has
119 increased due to infection by the fungi *Raffaelea quercivora* (Kobayashi and Ueda, 2005).
120 At present, the area ratio of broad-leaved forest to coniferous forest is approximately ten is
121 to one. The mixed temperate forest has a mean annual precipitation and average temperature
122 of 1385 mm and 14.9°C, respectively (Nara Prefecture; Nara Local Meteorological Office,
123 Japan), with an elevation from 120-210 m above sea level. To avoid errors arising from edge
124 effects (Wuyts et al., 2008), all samples were taken 60–120 m away from the forest edge.
125 The throughfall samples were collected at two sites in the mixed forest; a coniferous tree-
126 dominant forest (coniferous forest, site C) covered mostly by Japanese red pine and Japanese
127 cypress, and a broad-leaved tree-dominant forest (broad-leaved forest, site B) covered
128 mainly by Konara oak and sawtooth oak (*Quercus acutissima*). To check the spatial
129 heterogeneity of the sampling sites, sub samples were collected 250 m away from site C
130 which is composed of a coniferous tree-dominant forest (Site SC) from September to
131 November in 2016. The sampling sites for collection of throughfalls were located around
132 the central portion of both forest types. The average leaf area index (LAI), canopy openness

and canopy closure values were 1.8 ± 0.2 m^2 m^{-2}, $27.6 \pm 4.8\%$ and $78.9 \pm 6.7\%$ for the coniferous forest and 2.8 ± 0.7 m^2 m^{-2} , $13.4 \pm 3.8\%$ and $84.5 \pm 2.2\%$ for the broad-leaved forest, respectively. Rainfall without any canopy obstructions (site R) was located 100 m away from the mixed forest.

For the collection of stemflow, four major tree species with close to average 22.5-29.1 cm diameter at breast height (DBH) values in the Satoyama forests were selected to represent trees growing within the Satoyama: Japanese red pine (DBH: 27 cm) and Japanese cypress (DBH: 20 cm) representing coniferous trees, and Konara oak (DBH: 22 cm) and Japanese hill cherry (*Prunus serrulata*, DBH: 33 cm) representing broad-leaved trees, all frequently found in the Satoyama.

2.2. Sampling procedures and analyses

We collected rain samples to measure pH, electric conductivity (EC), and dissolved ion concentrations of the gross rainfall, throughfall, and stemflow in 19 out of 43 total rain events that occurred from June 13, 2016 to January 23, 2017. However, some samples were missing due to a typhoon and sample amounts insufficient for chemical analysis. Samples for DOC and EEM determination were collected four times during the same sampling period.

Throughfall was collected using a polyethylene bottle (ca. 120 mm tall, sampling area ca.

80 cm^2) placed under both coniferous and broad-leaved forest types. Rainfall at site R was collected using the same bottle type at ground level. Stemflow was collected by a sheet of pre-cleaned medical gauze (FC gauze, Hakujuji Co., Tokyo) wrapped around the tree trunks at 1.0 m height and connected to a polyethylene bottle (5 L volume). The medical gauze was pre-cleaned by boiling in pure water for 20 min and drying prior to use. Both medical gauze and sampling bottle were installed before rain events. Simultaneously, sampling bottles to collect throughfall and gross rainfall were placed both inside and outside the mixed forests. After a rain event stopped, rain samples were transferred to the laboratory. Hence, the throughfall, gross rainfall and stemflow rain samples were collected from one rain event. The collected samples were filtered through a PTFE 0.45-μm-pore size membrane filter (Omnipore, Merck, Darmstadt, Germany). The filtrates were stored in the dark at 4°C before analyses.

The concentrations of anions (Cl^-, NO_3^- and SO_4^{2-}) and cations (Na^+, K^+, Mg^{2+} and Ca^{2+}) were measured by an ion chromatograph (LaChrom Elite, Hitachi High-Tech, Tokyo). The limits of detection (LOD) of the ion chromatograph calculated by 3σ were Na^+ (0.03 mg L^{-1}), K^+ (0.05 mg L^{-1}), Mg^{2+} (0.03 mg L^{-1}), Ca^{2+} (0.06 mg L^{-1}), Cl^- (0.02 mg L^{-1}), NO_3^- (0.01 mg L^{-1}), and SO_4^{2-} (0.01 mg L^{-1}), respectively. The EC and pH of non-filtered samples were determined immediately using portable water quality meters (EC11, Kenis and LAQUA D-

50, Horiba, Kyoto, Japan). The concentrations of DOC were measured with a total organic carbon (TOC) analyzer (TOC-V, Shimadzu, Kyoto, Japan). EEM was measured with a fluorescence spectrophotometer (FR-6200, Jasco, Tokyo). EEM fluorescence spectra were obtained by collecting emission scans (λEm 300–550 nm, 1-nm intervals) at 5-nm excitation wavelength intervals between λEx 240 and 450 nm. UV–Vis absorbance spectra were collected prior to the measurement of EEM fluorescence spectra using a double-beam spectrophotometer (UV-2600, Shimadzu, Kyoto, Japan) in the wavelength range of 240–550 nm. Primary and secondary inner filter effects, Raman scattering, and Rayleigh-Tyndall scattering of the obtained EEM fluorescence spectra were corrected (Larsson et al., 2007). The EEM was characterized by a parallel factor analysis, PARAFAC (Stedmon et al., 2007, ; Stedmon and Bro 2008). The PARAFAC analysis was carried out to identify fluorescent components obtained by the EEM. We used the DOM Fluor v.1.7 Toolbox (University of Copenhagen) for MATLAB (R 2013a, MathWorks, Natick, MA, USA) to fit the PARAFAC model over a dataset comprising all rain water samples. The components were verified by a random initialization and split-half analysis (Stedmon and Bro, 2008).

2.3. Deposition flux

We roughly estimated the deposition flux of the Satoyama forest. We first calculated the

187 yearly gross rainfall (G: mm y^{-1}) by using the 5-year average (2015–2019) of precipitation
188 provided by the government offices of Nara Prefecture. The rain partitionings of throughfall,
189 rainfall interception, and stemflow were calculated as follows (Eqs 1-4). We estimated the
190 ratio of throughfall by obtaining the correlation between the canopy openness and the ratio
191 of throughfall to gross rainfall (Noguchi et al., 2007; Eqs 1 and 2).

192 $$R_b = 0.00496C_b + 0.620 \cdots (1)$$

193 $$R_c = 0.00231C_c + 0.734 \cdots (2)$$

194 Where, R_b, R_c, C_b and C_c represent the ratio of throughfall in the broad-leaved forest (-),
195 the ratio of throughfall in the coniferous forest (-), canopy openness of the broad-leaved
196 forest (%) and canopy openness of the coniferous forest (%), respectively.

197

198 The throughfall in the broad-leaved forest (T_b: mm y^{-1}) and in the coniferous forest (T_c:
199 mm y^{-1}) were calculated by Eq 3.

200

201 $$T_{b\ or\ c} = G \times R_{b\ or\ c} \cdots (3)$$

202 Where, G and $R_{b\ or\ c}$ show the yearly gross rainfall (G: mm y^{-1}) of the Satoyama and the
203 ratio of throughfall in the broad-leaved forest or in the coniferous forest, respectively.

204

205 The rainfall interception ratio was calculated as the average ratio of the interception loss
206 to the gross rainfall observed in the temperate forests of Japan (Toba and Ohta, 2005). The
207 interception ratios to the gross rainfall used in this study were 0.147 for the coniferous forest
208 and 0.210 for the broad-leaved forest. The rainfall interception in the coniferous forest (I_c:
209 mm y^{-1}) or in the broad-leaved forest (I_b: mm y^{-1}) were calculated by multiplying the rainfall
210 interception with the yearly gross rainfall in Satoyama forest (G: mm y^{-1}).
211 The stemflow (mm y^{-1}) was calculated by subtracting both the throughfall (mm y^{-1}) and
212 the rainfall interception (mm y^{-1}) from the gross rainfall (mm y^{-1}) as shown in Eq 4.
213
214 $$S_{b\ or\ c} = G - T_{b\ or\ c} - I_{b\ or\ c} \cdots (4)$$
215
216 Where, $S_{b\ or\ c}$, G, $T_{b\ or\ c}$ and $I_{b\ or\ c}$ indicate stemflow in the broad-leaved forest (mm y^{-1}) or
217 the coniferous forest (mm y^{-1}), gross rainfall in the Satoyama forest (mm y^{-1}), throughfall in
218 the broad-leaved forest (mm y^{-1}) or the coniferous forest (mm y^{-1}) and rainfall interception
219 in the broad-leaved forest (mm y^{-1}) or the coniferous forest (mm y^{-1}), respectively.
220 The average concentrations of the cations, anions, and DOC in the Satoyama forest
221 obtained herein were used for the calculation of each flux (g m^{-2} y^{-1}).
222

223 *2.4. Dissolution test of anions and cations from leaves and bark samples*

224 The amounts of anions and cations from tree leaves and bark samples were determined as
225 follows. First, 50 g L^{-1} of leaves or bark was added to pure water and left for 1 d at ambient
226 temperature (approx. 25°C). The leachate was then filtered through a PTFE 0.45-μm-pore
227 size membrane filter (Omnipore, Merck). The filtrates were stored in the dark at 4°C before
228 the analyses. The concentrations of anion and cation were measured by the above-cited ion
229 chromatography (LaChrom Elite Hitachi High-Tech).

230

231 *2.5. Data processing*

232 We performed a multiple comparison test among rain fractions with normal distribution.
233 When the rain fraction showed non-normal distribution, Kruskal-Wallis test was carried out
234 to detect statistical difference among rain fractions. Probability (p)-values <0.01 or <0.05
235 were considered significant. We used hemispherical canopy photographs of the forest to
236 calculate LAI and canopy openness, and imaging software, i.e., Gap Light Analyzer ver. 2.0
237 (Frazer et al., 1999) was applied to extract the canopy structure and gap light transmission.

238 The back trajectory calculation of each air mass was performed using the Centre for
239 Global Environmental Research (CGER) Meteorological Data Explorer (METEX) provided
240 by Japan's National Institute for Environmental Studies (CGER-METEX 2016).

241

242 **3. Results and Discussion**

243 *3.1. pH and concentrations of cations and anions*

244 The average pH values of the rainfall, the throughfalls and the stemflows were 5.90, 5.55-

245 5.56 and 3.74-5.27, respectively **(Table 1)**.

246 The concentrations of cations in the rainfall and the throughfalls in the coniferous and

247 broad-leaved forests are illustrated in **Fig. 2a**. The average concentrations of Na^+, K^+, Mg^{2+}

248 and Ca^{2+} in the rainfall and the throughfalls were 1.36-1.58 mg L^{-1}, 0.70-7.13 mg L^{-1}, 0.17-

249 0.33 mg L^{-1} and 0.92-1.20 mg L^{-1}, respectively. The average concentrations of Cl^-, NO_3^-

250 and SO_4^{2-} were 1.40–2.42 mg L^{-1}, 1.05–2.82 mg L^{-1}, and 1.42–2.61 mg L^{-1}, respectively

251 (**Fig. 2b**). To check the spatial heterogeneity of the sampling sites in this study, the anion

252 and cation concentrations of sub samples collected from site SC were compared to those

253 from site C. The average concentrations of anions, Na^+ and K^+ did not show statistical

254 difference between site C and site SC. The average concentrations of Mg^{2+} and Ca^{2+} in site

255 SC were 0.59 mg L^{-1} and 1.86 mg L^{-1}, which were higher than those of site C. However,

256 those values obtained from site SC were almost within the concertation range of Mg^{2+} and

257 Ca^{2+} in site C.

258 The average concentrations of cations in the stemflows are illustrated in **Fig. 3a**. The

ranges of the concentrations from four trees were 1.02–2.38 mg L^{-1} for Na^+, 1.84-10.9 mg L^{-1} for K^+, 0.21-0.60 mg L^{-1} for Mg^{2+} and 0.70-2.60 mg L^{-1} for Ca^{2+}. The average concentrations of amions in the stemflows were 1.72-5.70 mg L^{-1} for Cl^-, 0.19-2.31 mg L^{-1} for NO_3^- and 0.68-2.87 mg L^{-1} for SO_4^{2-} , respectively (**Fig. 3b**).

We estimated the sources of NO_3^- and SO_4^{2-} by calculating the non-sea salt sulfate (nss-SO_4^{2-}) in the rainfall. The range of the nss-SO_4^{2-} concentration in the rainfall was 0.46–3.36 mg L^{-1}, accounting for 91.2%–98.6% of the total SO_4^{2-} (0.47–3.69 mg L^{-1}). Thus, the forest was affected mainly by atmospheric deposition due to anthropogenic activities. The effect of sea spray on the forest can expected to be negligible because the study site is located approx. 30 km from the sea and is surrounded by mountains.

We performed a 5-day backward trajectory analysis to identify the source(s) of NO_3^- and SO_4^{2-}. In summer, the air masses flowing to the study site originated from the Pacific Ocean, the Sea of Japan, and regional emissions (**Fig. 4a**), whereas during the autumn to winter months, air masses to the forest come mainly from the Asian continent (**Fig. 4b**). The different sources of air masses were reflected in the chemical compositions of the rainfall, throughfall and stemflow. The average concentrations of Na^+, Cl^-, NO_3^-, and SO_4^{2-} in the rainfall and throughfall collected in the autumn and winter were 2.5–6.0 times higher than those collected during the summer ($p<0.01$ or $p<0.05$, **Table 2**). Notably, the NO_3^- and SO_4^{2-}

277 concentrations of the throughfall in the broad-leaved forest collected in the autumn to winter
278 months was 5–6 times higher than those in the summer ($p<0.01$). From autumn to winter,
279 the average concentration of SO_4^{2-} tended to increase in the following order: rainfall (1.84
280 mg L^{-1}) < throughfall in the coniferous forest (1.98 mg L^{-1}) < throughfall in the broad-
281 leaved forest (4.15 mg L^{-1}). Similarly, the concentration of NO_3^- increased in the order of
282 rainfall (1.31 mg L^{-1}) < throughfall in the coniferous forest (3.95 mg L^{-1}) < throughfall in
283 the broad-leaved forest (4.43 mg L^{-1}).

284 The dry deposition of various elements increases with an increasing LAI (Devlaeminck
285 et al., 2005). In our present investigation, the LAIs of the broad-leaved forest and the
286 coniferous forest were 2.8 m^2 m^{-2} and 1.8 m^2 m^{-2}, respectively; thus, the broad-leaved forest
287 was affected by significant dry deposition compared to the coniferous forest. This is
288 consistent with increases in the monthly concentrations of SO_4^{2-} in the air of Nara city (near
289 the study site) during autumn and winter. In the spring to summer months, the concentrations
290 of SO_4^{2-} are approx. 45–70 nmol m^{-3} (Matsumoto and Murano 1998). During autumn and
291 throughout the winter, the concentrations increase to around 60–140 nmol m^{-3} (Matsumoto
292 and Murano 1998). We suspect that the origin of air pollutants was mainly domestic
293 emissions during the spring and summer.

294 In contrast, from autumn to the winter months, the origin of air pollutants can be traced

295 mainly to both domestic and continental Asian sources (e.g., coal combustion) (Wang et al.,
296 2018). We also observed this enrichment from atmospheric depositions in the stemflow data
297 obtained in the present study, especially those of the Japanese hill cherry and Japanese red
298 pine trees (**Table 3**). However, the enrichment of the atmospheric deposition in the
299 stemflows compared to the throughfall was not clear. This is because the tree stems might
300 be less affected by atmospheric deposition compared to the tree canopies.
301
302 *3.2. Dissolved organic matter*
303 The average DOC concentrations were 1.9 mg L^{-1} for rainfall, 10.6 mg L^{-1} for the
304 throughfall in the broad-leaved forest, and 6.6 mg L^{-1} for the throughfall in the coniferous
305 forest (**Fig. 5**). Concerning the stemflows, the average DOC concentrations were 11.2 -26.8
306 mg L^{-1} (**Fig. 5**). The increasing DOC concentration in stemflow and throughfall might have
307 resulted from the accumulation of organic matter from bark, litter and fauna supplemented
308 by the presence of epiphytes attached on the trees (Stubbins et al., 2017). The average DOC
309 concentrations in the throughfall (6.6–10.6 mg L^{-1}) and stemflow (11.2–26.8 mg L^{-1}) were
310 both within the range of values reported for throughfalls (3–19 mg L^{-1}, Le Mellec et al.,
311 2010; Van Stan and Stubbins, 2018; Chen et al., 2019) and stemflows (6–332 mg L^{-1},
312 Stubbins et al., 2017; Van Stan and Stubbins, 2018).

313 Here, the average $SUVA_{254}$ ranges of the throughfalls and stemflows were 1.5–2.7 and
314 1.7–3.1 L mg^{-1} m^{-1}, respectively (**Fig. 6**). Although there was no significant difference
315 among all fractions, the $SUVA_{254}$ values of the throughfalls and stemflows tended to be high
316 compared to that of the rainfall (0.3 L mg^{-1} m^{-1}), indicating tree-DOM was rich in aromatic
317 organic matter compared to rainwater. The $SUVA_{254}$ of the throughfalls was close to those
318 reported for throughfalls (2.0–3.3 L mg^{-1} m^{-1}) and stemflows (1.6–5.1 L mg^{-1} m^{-1}, Stubbins
319 et al., 2017; Van Stan et al., 2017; Wagner et al., 2019). However, the $SUVA_{254}$ of the
320 throughfalls in the studied broad-leaved forest varied widely from 0.2 to 7.9 L mg^{-1} m^{-1},
321 indicating that the aromatic carbon content in the DOC fractured.
322 We performed PARAFAC analyses to identify fluorescent components obtained by the
323 EEM. The characteristics of the fluorescent components identified in this study are listed in
324 **Table 4** and illustrated in **Figs. 7** and **8**, respectively. Component 1 was derived from protein
325 contained in tyrosine (Coble et al., 1998). Components 2, 5, and 7 represent UV humic
326 compounds (Stedmon et al., 2003; Coble et al., 1998). Component 3 is humic-like and
327 derived from microbial and photochemical degradation (Stedmon et al., 2007). Component
328 4 is derived from protein contained in tryptophan (Coble et al., 1998), and component 6 is
329 protein-like (Sanchez et al., 2013). The results of the PARAFAC analyses demonstrated that
330 compared to the rainfall, the throughfall in the broad-leaved forest was enriched with humic

substances (components 2, 3, and 5) and protein derivatives (component 6) ($p<0.05$) (Fig. 8). The stemflows were enriched with humic substances (components 2, 3, and 5 for the Japanese cypress and the Konara oak) and protein derivatives (components 1, 4 and 6 for the Japanese cypress; component 6 for the Japanese red pine) compared to the rainfall ($p<0.05$). The correlation efficient for the seven components obtained by the PARAFAC analyses or at UV absorbance at 254 nm (a254) and the DOC concentration of each fraction are provided in **Table 5**. High correlations were revealed between DOC concentration and component 7 ($r = 0.964$, $p<0.05$) for the rainfall, components 3, 5 and a254 ($r = 0.969–0.989$, $p<0.05$) for the throughfalls in the coniferous forest, component 6 ($r = 0.958$, $p<0.05$) for the stemflows from the Japanese hill cherry, and components 5 and 6 ($r = 0.977–0.996$, $p<0.05$) for the stemflows from the Japanese red pine. Additionally, the stemflows from the Konara oak showed a loose positive correlation between the DOC concentration and components 2, 3, 5 and a254 ($r = 0.913–0.942$, $p<0.1$). Similarly, the DOC concentrations of the throughfall in the coniferous forest and the stemflows from the Konara oak were loosely correlated with component 2 ($r = 0.908$, $p<0.1$). We thus conclude that the DOC concentrations of the rainfalls were affected by humic substances. Regarding the stemflows from the Japanese hill cherry, the DOC concentration was controlled by protein derivatives. In the case of throughfall in the coniferous forest, the DOC concentrations were affected by humic

substances and a254 representing colored dissolved organic matter (CDOM), which has UV absorbance. For stemflow from the Konara oaks, DOC concentrations were affected by humic substances and CDOM with UV absorbance. For stemflow from Japanese red pines, DOC concentrations were affected by humic substances, protein derivatives, and CDOM with UV absorbance. The source of DOC is considered to be coming from the trees and supplemented by inputs from epiphytes and atmospheric deposition (Vanstan and Stubbins, 2018). As previously mentioned, this study site is affected by air masses from both the Asian continent and local emissions, therefore, atmospheric deposition is likely to be one of the contributors of humic substances as humic-like substances in aerosol accounts for 9-72% of water soluble organic matter (Zheng et al., 2013).

3.3. Deposition flux

Finally, we roughly estimated the deposition flux of the Satoyama forest (**Table 6**). The deposition flux of the DOC from the throughfalls (7.31–10.1 g m^{-2} y^{-1}) and stemflow (1.79–3.84 g m^{-2} y^{-1}) obtained in this study were within the range of values obtained from various temperate forest (4.1-34.0 g m^{-2} y^{-1} for throughfall; 0.1–5.6 g m^{-2} y^{-1} for stemflow; Van Stan and Stubbins, 2018). However, the deposition flux of the DOC from the stemflows obtained in this study was relatively higher than those of previous studies.

The deposition flux of cations and anions (except for K^+, Ca^{2+} and SO_4^{2-}) obtained in this study were close to those of coniferous and broad-leaved forests in Japan (Na^+: 1.7–2.4, K^+: 2.2–3.1, Mg^{2+}: 1.2–1.4, Ca^{2+}: 3.1–3.2, Cl^-: 3.4–5.3, NO_3^-: 2.6–6.0, SO_4^{2-}: 8.5–11.8 g m^{-2} y^{-1}, Oura, 2010). In contrast, the deposition flux of K^+ from broad-leaved forest in this study (8.35 g m^{-2} y^{-1}) was high compared to those of coniferous and broad-leaved forests in Japan. The high deposition flux of K^+ in the broad-leaved forest has been attributed to leaching from the canopy (Devlaeminck et al., 2005). We investigated the amounts of ions dissolved from the tree bark and leaves (**Table 7**) and found that the high amounts of K^+ were dissolved from the Konara oaks and Japanese hill cherry. The deposition flux of Ca^{2+} in the Satoyama forest was low compared to those of coniferous and broad-leaved forests in Japan. The deposition flux of SO_4^{2-} at the study site (1.78–2.58 g m^{-1} y^{-1}) was low compared to most Japanese forests (8.5–26.7 g m^{-1} y^{-1}, Oura, 2010; Kobayashi et al., 1999) and a forest in the San Bernardino Mountains, USA (4.8–29 g m^{-1} y^{-1}, Fenn et al., 2000) and relatively low compared to forests in Flanders, Belgium (2.6–10.6 g m^{-1} y^{-1}, Wuyts et al., 2008). The canopy openness of the Satoyama forest in this study was 13.4%–27.6%, which is higher than that of common natural forests worldwide. We thus considered the canopy interaction to be low compared to that in natural forests, resulting in low deposition flux of SO_4^{2-} in Satoyama forests. However, as previously mentioned, the traditional Japanese Satoyama is

385 now facing a serious crisis. In this study site, mass mortality of oak trees has been observed
386 widely. If the forest composition changes into the coniferous type from the present Satoyama
387 due to mass mortality of oak trees, the deposition flux of DOC and K^+ might decrease 33%
388 and 62% (**Table 6:** described in Coniferous forest/Present). One reason for the decrease of
389 the DOC deposition flux may be the decreased amount of pollen produced from oak trees.
390 It is reported that a large amount of pollen from oak trees significantly contributed to the
391 highest DOC concentration in throughfalls seen in the forests of Georgia and South Carolina
392 in the southeastern USA (Van Stan et al., 2017, Chen et al., 2019) and in New England
393 (Decina et al., 2018). In contrast, the deposition flux of NO_3^- might increase 20% due to
394 mass mortality of oak trees (**Table 6**). As described in **Table 2**, the main source of NO_3^- in
395 our study site is atmospheric deposition. Coniferous canopies show a higher filtering
396 capacity to atmospheric deposition than those of broadleaved ones because the structure of
397 twigs with needle shaped leaves favors deposition through impaction and diffusion
398 processes (Le Mellec et al., 2010), which is well consistent with the higher throughfall
399 depositions observed in coniferous forests in Germany (Rothe et al., 2002, Le Mellec et al.,
400 2010). Hence, the deposition flux of NO_3^- would favor the coniferous type trees due to mass
401 mortality of oak trees. Similar to our study site, the mass mortality of oak trees has been
402 observed worldwide such as in North America (Dey and Schweitzer et al., 2018), central

403 USA (Bendixsen et al., 2015, Wood et al., 2018) and southern Europe (Colangelo et al., 2018,
404 Etzold et al., 2019). Ultimately, the decrease of DOC deposition flux from those sites will
405 result in the decrease of riverine DOC fluxes into the coasts accompanied by changes in the
406 terrestrial and marine carbon cycles as DOC is an important source of humic substances with
407 chelating functions in river-ocean systems. Especially, organic Fe-binding ligands are
408 important substances in iron uptake for marine phytoplankton (Gledhill and Buck, 2012).
409 Furthermore, the increase of deposition flux of NO_3^- from those forests will lead to nitrogen
410 saturation, which in turn enhances the acidification of soils and leaching of nitrate into
411 surface and ground water. In the near future, the further deterioration of these forests might
412 change river-ocean linkages affecting forested catchments and aquatic ecosystems.
413

414 **4. Conclusions**

415 We characterized the chemical behaviors of major ions and DOM in the throughfalls and
416 stemflows in a typical Satoyama forest facing imminent deterioration located in Nara
417 Prefecture, Japan. The average DOC concentrations in the throughfall and stemflow in the
418 Satoyama site were both within the range of values reported elsewhere. The Satoyama forest
419 examined herein was affected by both atmospheric deposition due to anthropogenic
420 activities and by the seasonal changes in air masses. The deposition flux of sulfate in the

Satoyama forest was low compared to that in general forests. This is because the canopy interaction of the Satoyama forest was low compared to that of natural forests. If the forest composition eventually change into a pure coniferous forest from the present Satoyama mixed forest due to mass mortality of oak trees, the deposition flux of DOC and K^+ might decrease 33% and 62%, and NO_3^- might increase 20%. In the near future, the degradation of Satoyama landscapes might change DOC and nitrogen loads, resulting to imbalances in river-ocean linkages affecting forested catchments and aquatic ecosystems in Japan.

Acknowledgements

This study was supported in part by the Super Science High School Program (3036) provided by the Japan Science and Technology Agency. We also thank Michiko Kato, Hiroki Yamamoto, Mayu Inoue, Ayane Kawaguchi, Kentaro Onishi, and Moe Hirano for their help with the rain sampling and LAI measurements. Meteorological Data Explorer (METEX) was provided by Dr. Zeng Jiye (Centre for Global Environmental Research National Institute for Environmental Studies).

Declaration of interests

The authors declare that they have no known competing financial interests or personal

relationships that could have appeared to influence the work reported in this paper.

Authorship contribution statement

Satoshi ASAOKA : Conceptualization, Methodology, Formal analysis, Writing original draft, Supervision; Fuyuhiko SUMIKAWA: Conceptualization, Supervision; Yoshifumi WATANABE: Conceptualization, Supervision, Data quality checking; Waqar Azeem JADOON: Formal analysis; Masaki OHNO: Data processing; Shuto NOBUMICHI: Data processing; Yuki WAKAMATSU: Data processing; Lawrence M. LIAO: Data processing, English review; Akane KANAZAWA: Investigation, Formal analysis; Yuka SATO: Investigation, Formal analysis; Natsumi FUJIWARA: Investigation, Formal analysis

References

Bendixsen, D. P., Hallgren, S. W., & Frazier, A. E. (2015). Stress factors associated with forest decline in xeric oak forests of south-central United States. *Forest Ecology and Management*, 347, 40-48. https://doi.org/10.1016/j.foreco.2015.03.015

Cao, X., Aiken, G. R., Butler, K. D., Huntington, T. G., Balch, W. M., Mao, J., & Schmidt-Rohr, K. (2018). Evidence for major input of riverine organic matter into the ocean. *Organic Geochemistry*, 116, 62-76. https://doi.org/10.1016/j.orggeochem.2017.11.001

CGER (Centre for Global Environmental Research) METEX (Meteorological Data

458 Explorer). 2016. http://db.cger.nies.go.jp/metex/index.jp.html

459 Chen, H., Tsai, K. P., Su, Q., Chow, A. T., & Wang, J. J. (2019). Throughfall dissolved
460 organic matter as a terrestrial disinfection byproduct precursor. *ACS Earth Space*
461 *Chemistry*, 3(8), 1603-1613. https://doi.org/10.1021/acsearthspacechem.9b00088

462 Coble, P. G., Del Castillo, C. E., & Avril, B. (1998). Distribution and optical properties of
463 CDOM in the Arabian Sea during the 1995 Southwest Monsoon. *Deep Sea Research*
464 *Part II: Topical Studies in Oceanography*, 45(10-11), 2195-2223.
465 https://doi.org/10.1016/S0967-0645(98)00068-X

466 Colangelo, M., Camarero, J. J., Borghetti, M., Gentilesca, T., Oliva, J., Redondo, M. A., &
467 Ripullone, F. (2018). Drought and Phytophthora are associated with the decline of oak
468 species in southern Italy. *Frontiers in Plant Science*, 9, 1595.
469 https://doi.org/10.3389/fpls.2018.01595

470 Decina, S. M., Templer, P. H., & Hutyra, L. R. (2018). Atmospheric inputs of nitrogen,
471 carbon, and phosphorus across an urban area: Unaccounted fluxes and canopy
472 influences. *Earth's Future*, 6(2), 134-148. https://doi.org/10.1002/2017EF000653

473 Devlaeminck, R., De Schrijver, A., & Hermy, M. (2005). Variation in throughfall
474 deposition across a deciduous beech (*Fagus sylvatica* L.) forest edge in Flanders.
475 *Science of the Total Environment*, 337(1-3), 241-252.
476 https://doi.org/10.1016/j.scitotenv.2004.07.005

477 Dey, D. C., & Schweitzer, C. J. (2018). A review on the dynamics of prescribed fire, tree
478 mortality, and injury in managing oak natural communities to minimize economic loss

in North America. *Forests*, 9(8), 461.

FAO, Global forest resources assessment 2005: http://www.fao.org/3/a0400e/a0400e00.htm

Fenn, M. E., Poth, M. A., Schilling, S. L., & Grainger, D. B. (2000). Throughfall and fog deposition of nitrogen and sulfur at an N-limited and N-saturated site in the San Bernardino Mountains, southern California. *Canadian Journal of Forest Research*, 30(9), 1476-1488. https://doi.org/10.1139/x00-076

Etzold, S., Ziemińska, K., Rohner, B., Bottero, A., Bose, A. K., Ruehr, N. K., Zingg, A. & Rigling, A. (2019). One century of forest monitoring data in Switzerland reveals species-and site-specific trends of climate-induced tree mortality. *Frontiers in Plant Science*, 10, 307. https://doi.org/10.3389/fpls.2019.00307

Frazer, G.W., Canham, C.D., & Lertzman, K.P. (1999). Gap Light Analyzer (GLA): Imaging software to extract canopy structure and gap light transmission indices from true-colour fisheye photographs, users' manual and program documentation, Simon Fraser University, Burnaby, British Columbia, and the Institute of Ecosystem Studies, Millbrook, New York.

Gan, E., & Tsing, A. (2018). How things hold: A diagram of coordination in a Satoyama forest. *Social Analysis*, 62(4), 102-145. https://doi.org/10.3167/sa.2018.620406

Gledhill, M., & Buck, K. N. (2012). The organic complexation of iron in the marine environment: a review. *Frontiers in Microbiology*,3, 69. https://doi.org/10.3389/fmicb.2012.00069

500 Gomes, H. D. R., Xu, Q., Ishizaka, J., Carpenter, E. J., Yager, P. L., & Goes, J. I. (2018).
501 The influence of riverine nutrients in niche partitioning of phytoplankton
502 communities–a contrast between the Amazon River Plume and the Changjiang
503 (Yangtze) River diluted water of the East China Sea. *Frontiers in Marine Science*, 5,
504 343. https://doi.org/10.3389/fmars.2018.00343

505 Häder, D. P., & Barnes, P. W. (2019). Comparing the impacts of climate change on the
506 responses and linkages between terrestrial and aquatic ecosystems. *Science of the Total*
507 *Environment*, 682, 239-246. https://doi.org/10.1016/j.scitotenv.2019.05.024

508 Holtvoeth, J., Wagner, T., & Schubert, C. J. (2003). Organic matter in river‐influenced
509 continental margin sediments: The land‐ocean and climate linkage at the Late
510 Quaternary Congo fan (ODP Site 1075). *Geochemistry, Geophysics, Geosystems*,
511 4(12). https://doi.org/10.1029/2003GC000590

512 Indrawan, M., Yabe, M., Nomura, H., & Harrison, R. (2014). Deconstructing satoyama–
513 The socio-ecological landscape in Japan. *Ecological Engineering*, 64, 77-84.
514 https://doi.org/10.1016/j.ecoleng.2013.12.038

515 Ito, H. (2016). Changes in understory species occurrence of a secondary broadleaved forest
516 after mass mortality of oak trees under deer foraging pressure. *Peer J*, 4, e2816.
517 https://doi.org/10.7717/peerj.2816

518 Jiao, Y., Ding, Y., Zha, Z., & Okuro, T. (2019). Crises of biodiversity and ecosystem
519 services in Satoyama landscape of Japan: A review on the role of management.
520 *Sustainability*, 11(2), 454. https://doi.org/10.3390/su11020454

521 Kamada, M. (2017). Satoyama Landscape of Japan—Past, Present, and Future. In

522 Landscape ecology for sustainable society (pp. 87-109). Springer, Cham.

523 Kamiyama, C., Hashimoto, S., Kohsaka, R., & Saito, O. (2016). Non-market food
524 provisioning services via homegardens and communal sharing in satoyama socio-
525 ecological production landscapes on Japan's Noto peninsula. *Ecosystem Services*, 17,
526 185-196. https://doi.org/10.1016/j.ecoser.2016.01.002

527 Katoh, K., Sakai, S., & Takahashi, T. (2009). Factors maintaining species diversity in
528 Satoyama, a traditional agricultural landscape of Japan. *Biological Conservation*,
529 142(9), 1930-1936. https://doi.org/10.1016/j.biocon.2009.02.030

530 Kobayashi, M., & Ueda, A. (2005). Wilt disease of Fagaceae trees caused by *Platypus*
531 *quercivorus* (Murayama) (Coleoptera: Platypodidae) and the associated fungus: Aim is
532 to clarify the damage factor. *Journal of the Japanese Forest Society,* 87(5), 435-450. in
533 Japanese with English abstract. https://doi.org/10.4005/jjfs.87.435

534 Kobayashi, T., Nakagawa, Y., Tamaki, M., Hiraki, T., Aikawa, M., & Shoga, M. (1999).
535 Estimation of acid deposition to forest canopies via cloud water by means of
536 throughfall measurements and cloud water collection – Measurements in *Cryptomeria*
537 *japonica* stands at Mt. Rokko in Kobe, western Japan. *Environmental Science,* 12(4),
538 399-411. in Japanese with English abstract.

539 Koganezawa, T. (2016). Development of region by using of the ecosystem service in
540 Satoyama, Satochi, Satoumi. *Bulletin of the Society of Sea Water Science, Japan* 70,
541 217-226. in Japanese with English abstract. https://doi.org/10.11457/swsj.70.4_217

542 Larsson, T., Wedborg, M., & Turner, D. (2007). Correction of inner-filter effect in

543 fluorescence excitation-emission matrix spectrometry using Raman scatter. *Analytica*
544 *Chimica. Acta*, 583(2), 357-363. https://doi.org/10.1016/j.aca.2006.09.067

545 Le Mellec, A., Meesenburg, H., & Michalzik, B. (2010). The importance of canopy-
546 derived dissolved and particulate organic matter (DOM and POM) – Comparing
547 throughfall solution from broadleaved and coniferous forests. *Annals of Forest Science*,
548 67(4), 411. https://doi.org/10.1051/forest/2009130

549 Matsumoto, M., & Murano, K. (1998). Estimation of dry deposition to trees etc. by
550 inferential method and a discussion for forest damage – Observation throughout the
551 years in Nara city. *Journal of the Chemical Society of Japan*, 7, 495-505.
552 https://doi.org/10.1246/nikkashi.1998.495

553 Muller, F. L. L. (2018). Exploring the potential role of terrestrially derived humic
554 substances in the marine biogeochemistry of iron. *Frontiers in Earth Science*, 6, 159.
555 https://doi.org/10.3389/feart.2018.00159

556 Nakajima, H. (2019) Region-wide mass mortality of Japanese oak due to ambrosia beetle
557 infestation: Mortality factors and change in oak abundance. *Forest Ecology and*
558 *Management*, 449, 117468. https://doi.org/10.1016/j.foreco.2019.117468

559 Nara Local Meteorological Office, Japan: https://www.jma-net.go.jp/nara/ (Accessed on
560 16th Jun 2021)

561 Noguchi, S., Yasuda, Y., & Murakami, W. (2007). Comparison of throughfall at
562 *Cryptomeria japonica* and *Fagus crenata* stands in FFPRI Tohoku research center.
563 *Bulletin of the Forestry and Forest Products Research Institute*, 6(3), 157-162. (in

564 Japanese with English abstract)

565 Oura, N., (2010). Effect of nitrogen deposition on nitrogen cycling in forested ecosystems
566 and N_2O emission from the forest floor. *Bulletin of National Institute for Agro-*
567 *Environmental Sciences*. 27, 1-84.

568 Rothe, A., Huber, C., Kreutzer, K., & Weis, W. (2002). Deposition and soil leaching in
569 stands of Norway spruce and European beech: results from the Höglwald research in
570 comparison with other European case studies. *Plant and Soil*, 240(1), 33-45.

571 Sanchez, N. P., Skeriotis, A. T., & Miller, C. M. (2013). Assessment of dissolved organic
572 matter fluorescence PARAFAC components before and after coagulation – Filtration in
573 a full scale water treatment plant. *Water Research*, 47(4), 1679-1690.
574 https://doi.org/10.1016/j.watres.2012.12.032

575 Stedmon, C.A, Markager S., & Bro R. (2003). Tracing dissolved organic matter in aquatic
576 environments using a new approach to fluorescence spectroscopy. *Marine Chemistry,*
577 82(3-4), 239-254. https://doi.org/10.1016/S0304-4203(03)00072-0

578 Stedmon, C. A., Markager, S., Tranvik, L., Kronberg, L., Slätis, T., & Martinsen, W.
579 (2007). Photochemical production of ammonium and transformation of dissolved
580 organic matter in the Baltic Sea. *Marine Chemistry*, 104(3-4), 227-240.
581 https://doi.org/10.1016/j.marchem.2006.11.005

582 Stedmon, C. A., & Bro, R., (2008). Characterizing dissolved organic matter fluorescence
583 with parallel factor analysis: A tutorial. *Limnology and Oceanography: Methods*, 6(11),
584 572-579. https://doi.org/10.4319/lom.2008.6.572

585 Stubbins, A., Silva, L. M., Dittmar, T., & Van Stan, J. T. (2017). Molecular and optical
586 properties of tree-derived dissolved organic matter in throughfall and stemflow from
587 live oaks and eastern red cedar. *Frontiers in Earth Science*, 5, 22.
588 https://doi.org/10.3389/feart.2017.00022

589 Takeuchi, K. (2010). Rebuilding the relationship between people and nature: The
590 Satoyama Initiative. *Ecological Research*, 25(5), 891-897

591 Toba, T., & Ohta, T. (2005). An observational study of the factors that influence
592 interception loss in boreal and temperate forests. *Journal of Hydrology*, 313(3-4), 208-
593 220. https://doi.org/10.1016/j.jhydrol.2005.03.003

594 Van Stan, J. T., & Stubbins, A. (2018). Tree-DOM: Dissolved organic matter in throughfall
595 and stemflow. *Limnology and Oceanography. Letters*, 3(3), 199-214.
596 https://doi.org/10.1002/lol2.10059

597 Van Stan, J. T., Wagner, S., Guillemette, F., Whitetree, A., Lewis, J., Silva, L., & Stubbins,
598 A. (2017). Temporal dynamics in the concentration, flux, and optical properties of tree-
599 derived dissolved organic matter in an epiphyte-laden oak-cedar forest. *Journal of*
600 *Geophysical Research: Biogeosciences*, 122(11), 2982-2997.
601 https://doi.org/10.1002/2017JG004111

602 Wagner, S., Brantley, S., Stuber, S., Van Stan, J., Whitetree, A., & Stubbins, A. (2019).
603 Dissolved black carbon in throughfall and stemflow in a fire-managed longleaf pine
604 woodland. *Biogeochemistry*, 146(2), 191-207. https://doi.org/10.1007/s10533-019-
605 00620-2

606 Wang, Z., Zheng, F., Zhang, W., & Wang, S. (2018). Analysis of SO_2 pollution changes of
607 Beijing-Tianjin-Hebei region over China based on OMI observations from 2006 to
608 2017. *Advances Meteorology*, 2018. https://doi.org/10.1155/2018/8746068

609 Washitani, I. (2001). Traditional sustainable ecosystem 'SATOYAMA' and biodiversity
610 crisis in Japan: Conservation ecological perspective. *Global Environmental Research*,
611 5, 119-133.

612 Wood, J. D., Knapp, B. O., Muzika, R. M., Stambaugh, M. C., & Gu, L. (2018). The
613 importance of drought–pathogen interactions in driving oak mortality events in the
614 Ozark Border Region. *Environmental Research Letters*, 13(1), 015004.

615 Wuyts, K., De Schrijver, A., Staelens, J., Gielis, L., Vandenbruwane, J., & Verheyen, K.
616 (2008). Comparison of forest edge effects on throughfall deposition in different forest
617 types. *Environmental Pollution*, 156(3), 854-861.
618 https://doi.org/10.1016/j.envpol.2008.05.018

619 Zheng, G., He, K., Duan, F., Cheng, Y., & Ma, Y. (2013). Measurement of humic-like
620 substances in aerosols: A review. *Environmental Pollution*, 181, 301-314.
621 https://doi.org/10.1016/j.envpol.2013.05.055

622

623

624

Figures

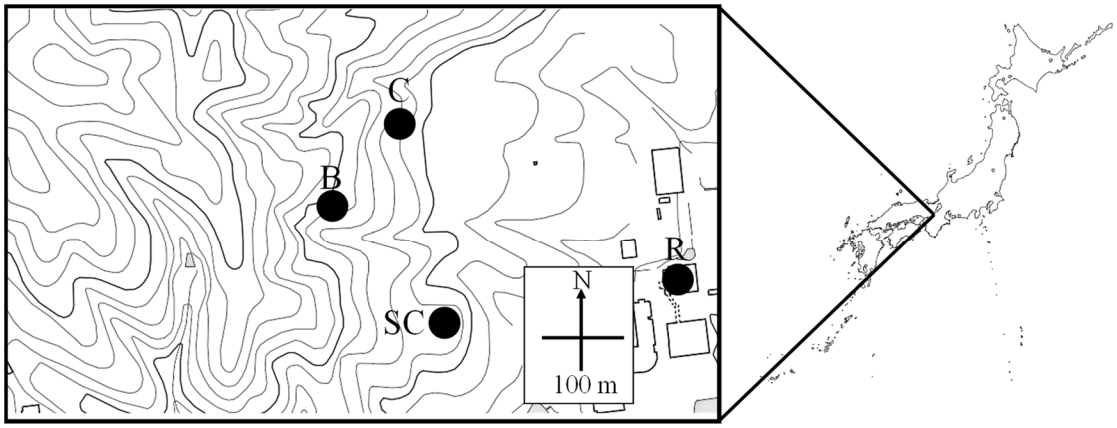

Map was drawn using GSI Vector provided by Geospatial Information Authority of Japan with appropriate modification.

Fig. 1 Study sites of Satoyama forest.

Site R: rainfall sampling site; Site B: throughfall sampling site in the broad-leaved forest; C: throughfall sampling site in the coniferous forest; SC: throughfall sub sampling site in the coniferous forest

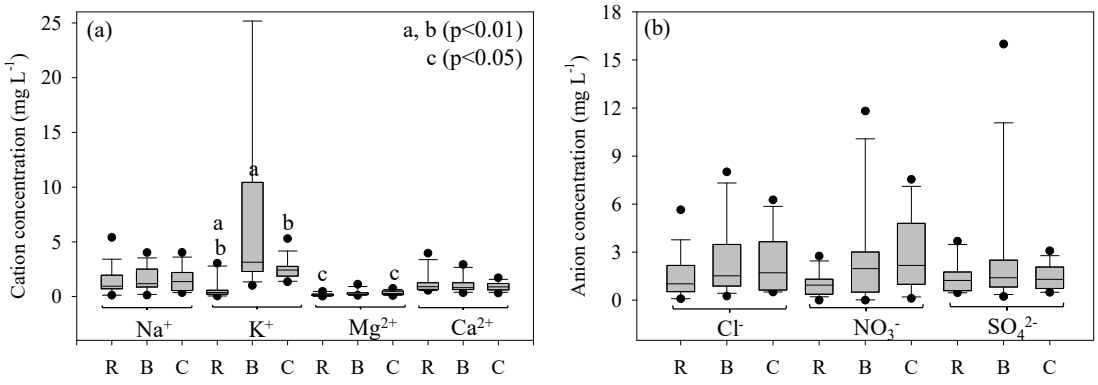

Fig. 2 Cation (a) and anion (b) concentrations of rainfall and throughfall.

B: throughfall in the broad-leaved forest, C: throughfall in the coniferous forest, R: rainfall

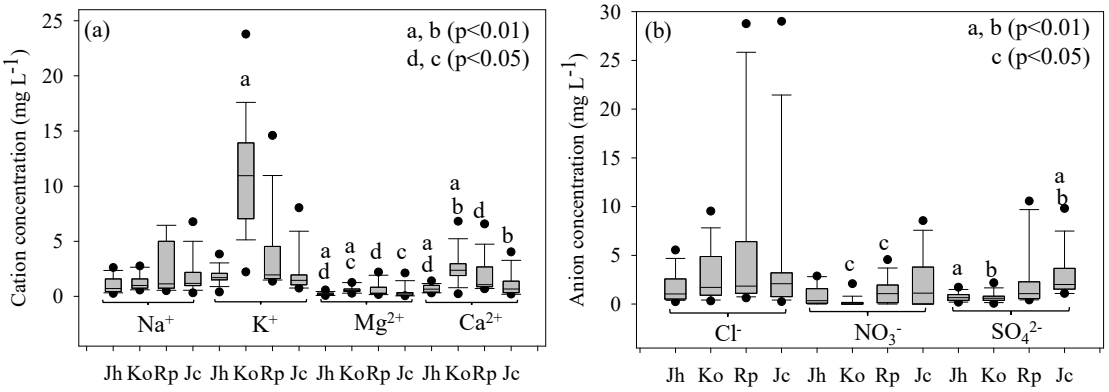

Fig. 3 Cation (a) and anion (b) concentrations of stemflow.

Jc: stemflow from Japanese cypress, Jh: stemflow from Japanese hill cherry, Ko: stemflow from Konara oak, Rp: stemflow from Japanese red pine

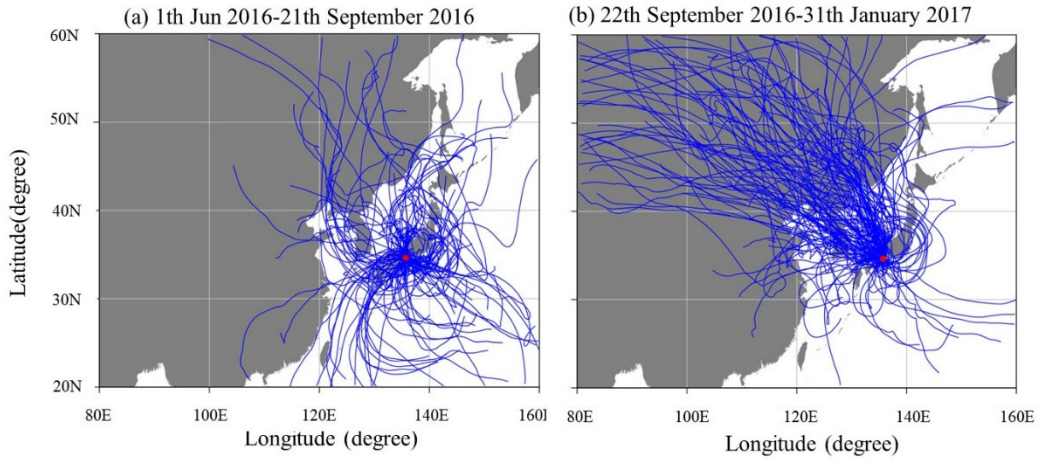

Fig. 4 The 5-day backward trajectory of the air mass at the study site calculated by CGER-METEX.

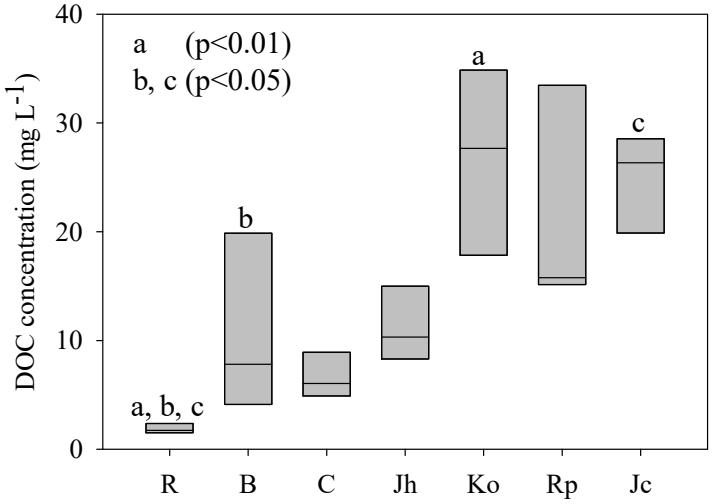

Fig. 5 Dissolved organic carbon (DOC) concentrations of rainfall, throughfalls and stemflows.
R:rainfall; B: throughfall in the broad-leaved forest, C: throughfall in the coniferous forest, Jc: stemflow from Japanese cypress, Jh: stemflow from Japanese hill cherry, Ko: stemflow from Konara oak, R: rainfall, Rp: stemflow from Japanese red pine

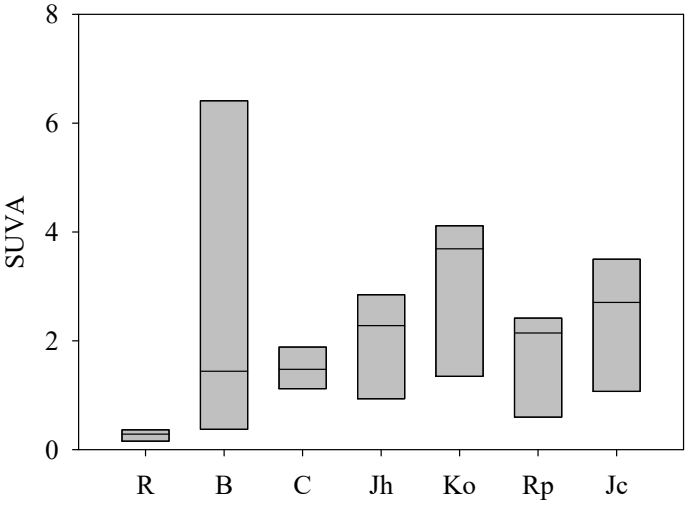

Fig. 6 $SUVA_{254}$ of rainfall, throughfall and stemflow.

B: throughfall in the broad-leaved forest, C: throughfall in the coniferous forest, Jc: stemflow from Japanese cypress, Jh: stemflow from Japanese hill cherry tree, Ko: stemflow from Konara oak, R: rainfall, Rp: stemflow from Japanese red pine.

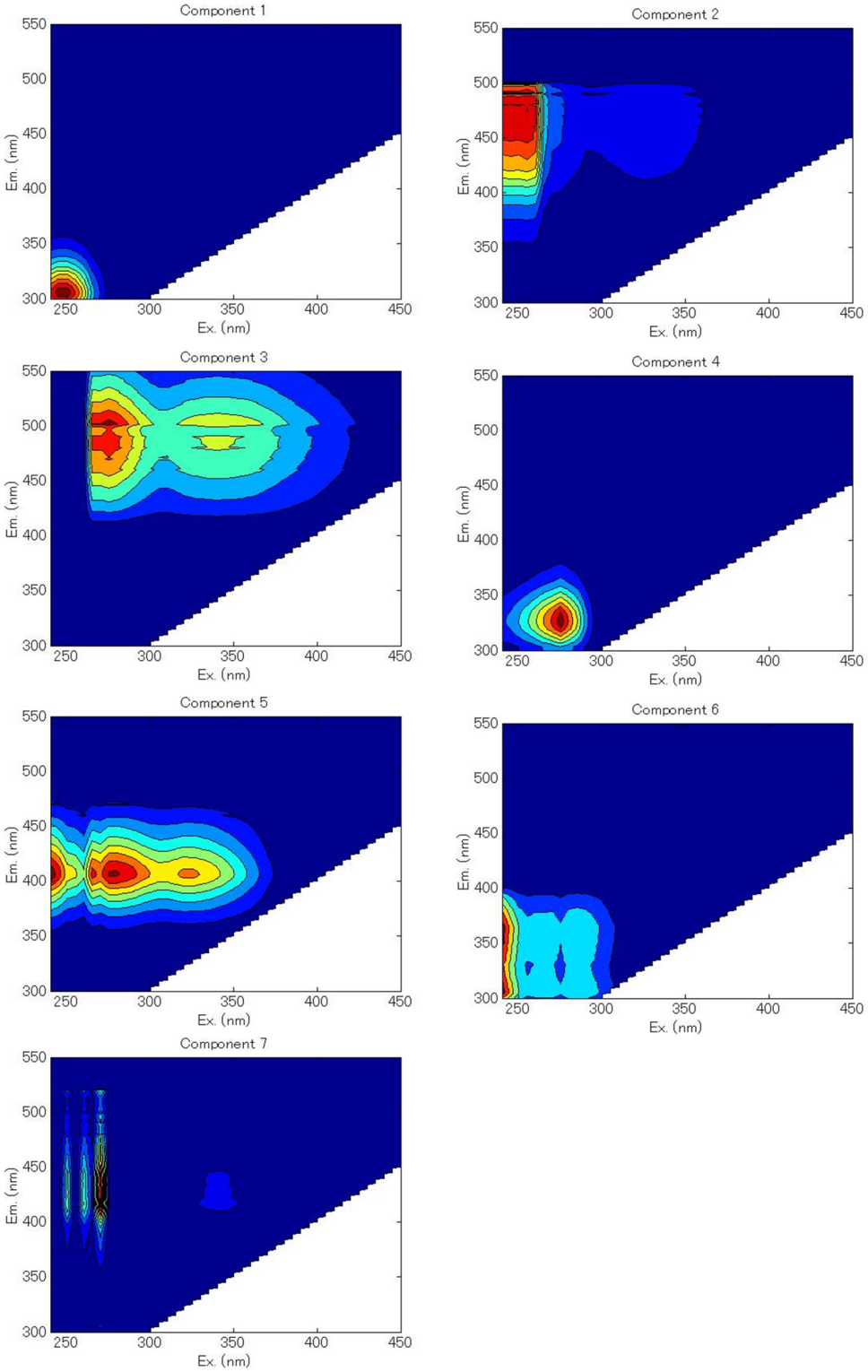

Fig. 7 The spectral properties of the seven fluorescent components identified by the PARAFAC analysis.

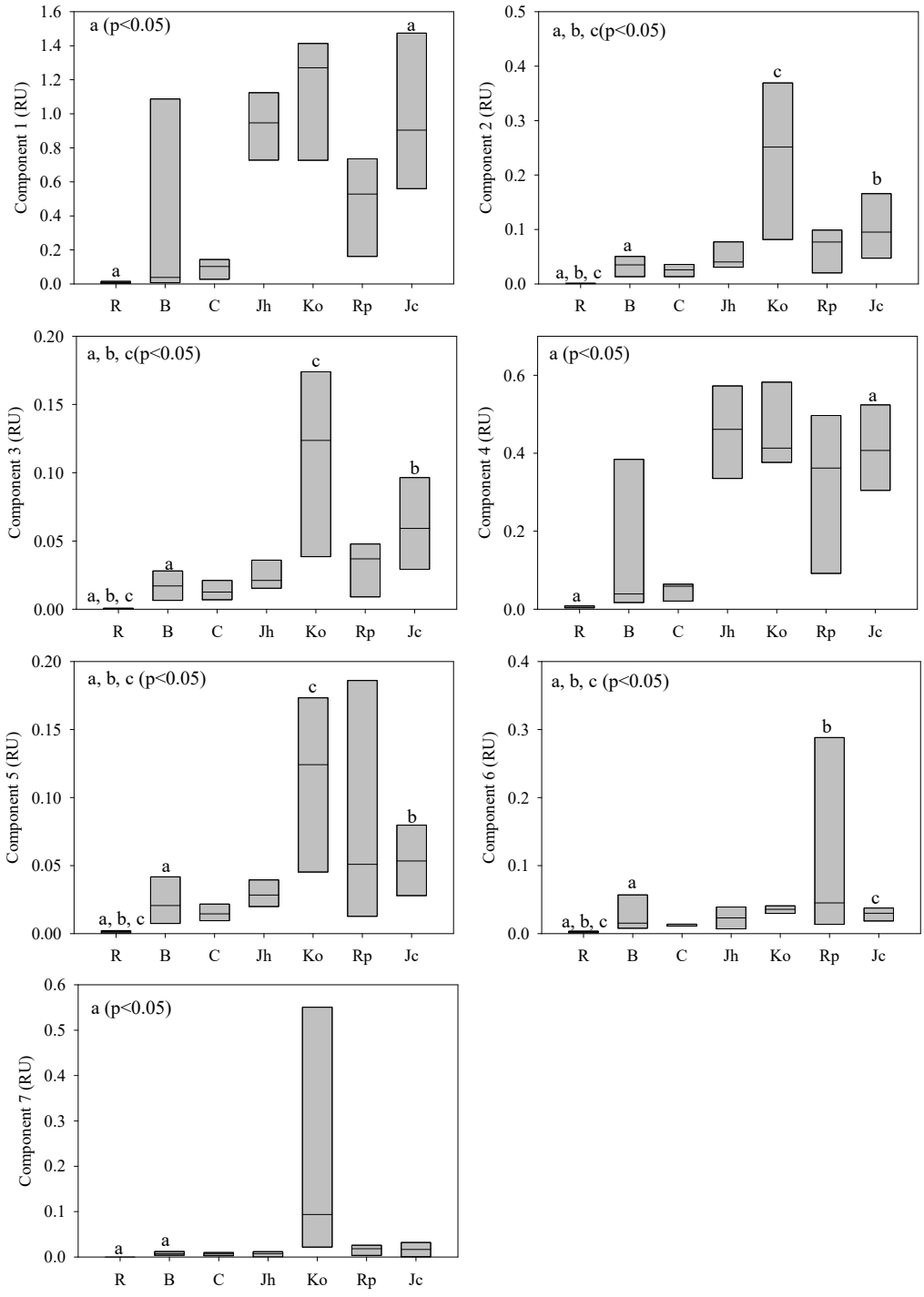

Fig. 8 The Raman unit fluorescence intensity of rainfall and throughfall, stemflow of each EEM components obtained by PARAFAC analyses

B: throughfall in the broad-leaved forest, C: throughfall in the coniferous forest, Jc: stemflow from Japanese cypress, Jh: stemflow from Japanese hill cherry tree, Ko: stemflow from Konara oak, R: rainfall, Rp: stemflow from Japanese red pine.

Tables

Table 1 pH and electro conductivity of each fraction

	pH		EC (mS m^{-1})	
Rain samples	AV.	SD	AV.	SD
Rainfall	5.90	0.55	1.80	1.69
TF in the broad-leaved forest	5.55	0.58	3.48	2.77
TF in the coniferous forest	5.56	0.66	3.24	2.10
SF from Japanese hill cherry	5.07	0.61	2.30	1.17
SF from Konara oak	5.27	0.61	4.87	2.11
SF from Japanese red pine	4.77	0.55	6.74	8.88
SF from Japanese cypress	3.74	0.36	10.5	7.76

TF: throughfall; SF:stemflow

Table 2 Cation and anion concentrations of rainfall and throughfall

	Rainfall						Throughfall in the broad-leaved forest						Throughfall in the coniferous forest					
	Summer		Autumn-Winter				Summer		Autumn-Winter				Summer		Autumn-Winter			
Ion	Av. (mg L^{-1})	SD	Av. (mg L^{-1})	SD	Ratio	p-value	Av. (mg L^{-1})	SD	Av. (mg L^{-1})	SD	Ratio	p-value	Av. (mg L^{-1})	SD	Av. (mg L^{-1})	SD	Ratio	p-value
Na^{+}	0.44	0.34	1.82	1.35	4.1	<0.01	0.73	0.42	2.22	1.07	3.1	<0.01	0.67	0.38	2.23	1.01	3.4	<0.01
K^{+}	0.24	0.23	0.93	1.02	3.9	-	3.07	1.78	10.6	11.1	3.5	-	2.63	1.41	2.35	0.50	1.1	-
Mg^{2+}	0.06	0.04	0.22	0.14	3.7	<0.01	0.19	0.07	0.42	0.34	2.3	-	0.18	0.07	0.44	0.18	2.4	<0.01
Ca^{2+}	0.71	0.18	1.45	1.12	2.0	-	0.72	0.27	1.38	0.90	1.9	-	0.73	0.27	1.38	0.90	1.9	<0.05
Cl^{-}	0.34	0.24	1.94	1.46	5.7	<0.01	0.94	0.54	3.68	2.72	3.9	<0.05	0.81	0.45	3.34	1.89	4.1	<0.01
NO_3-	0.52	0.22	1.31	0.79	2.5	<0.05	0.73	0.82	4.43	3.84	6.0	<0.01	1.31	0.96	3.95	2.53	3.0	<0.05
SO_4^{2-}	0.57	0.13	1.84	0.94	3.2	<0.01	0.82	0.42	4.15	5.30	5.0	<0.01	0.71	0.20	1.98	0.62	2.8	<0.01

Ratio: Autumn-Winter/Summer

Table 3 Cation and anion concentrations of stemflow

	Japanese hill cherry						Konara oak						Japanese red pine						Japanese cypress					
	Summer		Autumn-Winter				Summer		Autumn-Winter				Summer		Autumn-Winter				Summer		Autumn-Winter			
Ion	Av. (mg L^{-1})	SD	Av. (mg L^{-1})	SD	Ratio	p-value	Av. (mg L^{-1})	SD	Av (mg L^{-1})	SD	Ratio	p-value	Av. (mg L^{-1})	SD	Av. (mg L^{-1})	SD	Ratio	p-value	Av. (mg L^{-1})	SD	Av. (mg L^{-1})	SD	Ratio	p-value
Na^{+}	0.54	0.24	1.63	0.75	3.0	<0.01	1.00	0.61	1.60	0.65	1.6	-	1.33	1.65	3.56	2.40	2.7	<0.01	1.25	0.60	2.64	2.38	2.1	-
K^{+}	1.94	0.94	1.72	0.50	0.9	-	8.92	3.94	13.49	5.36	1.5	-	3.55	4.32	3.84	2.90	1.1	-	1.50	0.66	2.80	2.96	1.9	-
Mg^{2+}	0.16	0.11	0.29	0.15	1.8	<0.05	0.57	0.29	0.65	0.28	1.1	-	0.34	0.19	0.90	0.77	2.6	-	0.20	0.13	0.60	0.85	3.0	-
Ca^{2+}	0.61	0.34	0.81	0.29	1.3	-	2.42	1.88	2.84	0.99	1.2	-	1.81	1.88	2.05	1.32	1.1	-	0.84	0.73	1.35	1.51	1.6	-
Cl^{-}	0.99	0.89	2.67	1.79	2.7	<0.05	1.33	1.12	4.81	3.16	3.6	<0.05	1.60	1.20	10.30	11.00	6.4	<0.05	1.59	1.11	9.08	11.7	5.7	-
NO_3^{-}	0.52	0.90	1.17	1.03	2.2	-	0.32	0.67	0.04	0.10	0.1	-	1.26	0.77	1.40	1.79	1.1	-	3.76	2.58	<0.01	0	<0.002	<0.01
SO_4^{2-}	0.49	0.25	1.06	0.40	2.1	<0.01	0.51	0.21	0.90	0.70	1.8	-	0.87	0.55	3.86	3.92	4.4	<0.05	2.26	1.14	3.85	3.42	1.7	-

Table 4 Characteristics of the components identified by PARAFAC analyses

Components	Excitation (nm)	Emission (nm)	Characteristics	References
1	250	306	Tyrosine-like, Protein-like	Coble, 1998
2	255	475	UV-humic	Coble, 1998
3	275	501	Humic-like derived from microbial or photochemical degradation	Stedmon et al., 2007; Coble, 1998
4	275	327	Tryptophan-like, Protein-like	Coble, 1998
5	240	406	UV humic-like	Coble, 1998
6	240	363	Protein like	Sanchez et al., 2013
7	270	417	UV humic-like, Photoproduct of terrestrially derived DOM	Coble, 1998; Stedmon et al., 2007

Table 5 The correlation efficient between 7 components obtained by PARAFC analyses or UV absorbance at 254 nm (a 254) and DOC concentration of each fraction

Components	Characteristics	Rainfall	Throughfall		Stemflow			
			Broad-leaved forest	Coniferous forest	Japanese hill cherry	Konara oak	Japanese red pine	Japanese cypress
1	Tyrosine-like, Protein-like	-0.013	-0.514	0.629	0.397	-0.864	0.547	0.209
2	UV-humic	0.365	-0.612	0.908*	0.008	0.919*	0.325	0.476
3	Humic-like derived from microbial and photochemical degradation	0.428	-0.582	0.969**	-0.324	0.920*	0.606	0.450
4	Tryptophan-like, Protein-like	0.130	-0.536	0.526	0.395	-0.467	0.578	0.508
5	UV humic-like	0.815	-0.656	0.975**	0.144	0.913*	0.977**	0.553
6	Protein like	0.534	-0.638	-0.607	0.958**	-0.916*	0.996**	0.550
7	UV humic-like, Photoproduct of terrestrially derived DOM	0.964**	-0.428	0.857	-0.562	0.767	0.651	0.287
a254	CDOM with UV absorbance	0.497	-0.559	0.989**	-0.678	0.942*	0.910*	0.180

**p<0.05; *:p<0.1

Table 6 Deposition flux of DOC, cations and anions in Satoyama forest

flux ($g\ m^{-2}\ y^{-1}$)	DOC	Na^+	K^+	Ca^{2+}	Mg^{2+}	Cl^-	NO_3^-	SO_4^{2-}
Throughfall in the broad-leaved forest	10.1	1.45	6.78	0.30	1.02	2.30	2.59	2.48
Stemflow of broad-leaved trees	3.84	0.18	1.57	0.09	0.37	0.41	0.03	0.10
Total of broad-leaved forest	13.9	1.64	8.35	0.38	1.39	2.71	2.62	2.58
Throughfall in the coniferous forest	7.31	1.75	2.73	0.37	1.02	2.50	3.11	1.58
Stemflow of coniferous trees	1.79	0.16	0.22	0.04	0.11	0.39	0.14	0.20
Total of coniferous forest	9.10	1.91	2.95	0.40	1.14	2.89	3.25	1.78
Total of Satoyama forest (Present)	13.5	1.66	7.86	0.39	1.37	2.72	2.68	2.51
Coniferous forest/Present	0.67	1.1	0.38	1.0	0.83	1.1	1.2	0.71

Table 7 Amounts of cations and anions dissolved from bark or leaves (μg g^{-1})

		Na^+	SD	K^+	SD	Mg^{2+}	SD	Ca^{2+}	SD	Cl^-	SD	NO_3^-	SD	SO_4^{2-}	SD
Japanese hill cherry	bark	27.2	6.9	62.2	9.0	4.0	0.7	18.8	1.4	28.5	5.7	11.5	7.1	13.5	2.9
	leaf	22.6	20.3	500	80.5	35.2	20.4	19.1	17.4	69.2	70.1	2.1	5.0	8.8	3.4
Konara oak	bark	30.4	7.6	148	46.8	14.4	2.6	54.9	26.0	23.6	2.3	10.8	10.7	18.5	5.0
	leaf	48.4	9.6	289	91.1	11.3	0.8	54.1	7.4	40.8	7.6	18.9	2.1	25.6	6.3
Japanese red pine	bark	34.5	14.3	10.5	11.9	4.8	4.4	20.3	9.4	45.0	42.7	25.3	35.2	8.8	1.8
	leaf	22.8	4.9	37.4	9.6	2.3	0.3	13.3	3.9	17.2	3.5	17.1	7.0	8.3	1.5
Japanese cypress	bark	32.6	3.8	20.7	8.1	3.2	0.2	22.7	5.3	24.4	3.0	7.6	6.0	12.7	3.6
	leaf	39.9	12.7	75.9	29.4	4.2	0.7	22.6	7.2	37.0	11.4	30.9	7.0	14.7	3.0